Bubble Wall Profiles With More Than One Scalar Field: A Numerical Approach

Peter John*

Institut für Theoretische Physik, Universität Heidelberg, Philosophenweg 16, D-69120 Heidelberg, Germany
(October 14, 2018)

We present a general numerical approach to solve the equations for bubble wall profiles in models with more than one scalar field and CP violating phases. We discuss the algorithm as well as several problems associated with it and show some profiles for demonstration found with our method.

For the emergence of a baryon asymmetry of the Universe the Sakharov conditions necessarily demand deviation from thermodynamical equilibrium. This condition is fulfilled in first order phase transitions. They take place via nucleation of bubbles separating the symmetric from the broken phase. A first order phase transition might occur at temperatures around the electroweak scale. It turned out that in the Standard Model (SM) there is no phase transition at all for Higgs masses larger than 72 GeV [1]. Baryon number generation at the electroweak scale therefore requires more complicated models with additional light scalar fields such as Two-Higgs-doublet models (2HDM), MSSM, NMSSM or further extensions of the SM. In the MSSM there is a window for electroweak baryogenesis and an upper bound for the Higgs mass of about $m_H < 105$ GeV with a light stop of mass $m_{\tilde{t}_R} < m_{top}$ [2–6]. In the NMSSM the bounds on the Higgs mass are even weaker [7,8].

Having established the existence of a first order phase transition one can start the actual calculation of the baryon asymmetry itself. There are several mechanisms described in the literature [9–12]. All of them need the knowledge of the profile of the bubble wall during the phase transition. The kink ansatz in many situations is a good approximation but it might be interesting to have a more refined description and to determine which deviations occur in the presence of potentials depending on two or more Higgs fields and one or more CP violating phases [13–16]. In fact it turns out that the most important value in the MSSM is the deviation $\Delta\beta = max_v[v(\beta(v) - \beta(v_c))]/v_c$ from the straight line between the minima since the baryon asymmetry is [17,18] proportional to

$$I = \int_{-\infty}^{\infty} dx \frac{v^2(x)}{T_c^2} \frac{d\beta(x)}{dx} \qquad (1)$$

$\tan\beta = \frac{v_2}{v_1}$, $v^2(x) = v_1^2(x) + v_2^2(x)$. Having the exact profile one can calculate the baryon asymmetry like [17]

---

*e-mail: P.John@thphys.uni-heidelberg.de

and investigate the dynamics of expanding bubbles as in refs. [19–21].

To determine the bubble wall profile beyond a simple ansatz we have to solve the equations of motion numerically. In the case of more than one scalar field this is a highly nontrivial task since simple methods like overshooting-undershooting which work fine in the case of one scalar field like overshooting-undershooting fail. So one has to use methods which, beginning with an ansatz, converge to the actual solution. They are sometimes called "relaxation methods". Their practical implementation often is quite nontrivial. The issue of this letter is to present a working algorithm for the computation of bubble wall profiles.

We first have to find the equations of motion. In field theory they can be derived via Euler Lagrange equations from the Lagrangian density which has the general form

$$\mathcal{L} = (D_\mu \Phi_i)^+ (D^\mu \Phi_i) + V(\Phi_i, T) \qquad (2)$$

for several Higgs fields Φ_i (plus phases). Here D_μ is a covariant derivative and V denotes the effective potential. The equations of motion also can be derived thermodynamically similar to [19].

Let us consider the MSSM where we may have two dynamical Higgs scalars (or others as a light right-handed stop [2–6]) plus one CP violating phase θ. Using the real neutral field components ϕ_1, ϕ_2 and a relative phase θ the corresponding classical (tree level) Higgs potential is

$$V_{tree} = \frac{1}{2}m_1^2\phi_1^2 + \frac{1}{2}m_2^2\phi_2^2 + m_{12}^2\phi_1\phi_2\cos\theta$$
$$+ \frac{1}{32}(g^2 + g'^2)(\phi_1^2 - \phi_2^2)^2. \qquad (3)$$

In the MSSM the phase θ also enters the stop mass matrix.

To describe the phase transition we use the resummed one loop finite temperature effective potential (see e.g. ref. [22])

$$V_T = V_{tree} + V_1(T = 0) + V_1(T \neq 0) + V_{Daisy}. \qquad (4)$$

For the bubble wall in the MSSM without CP violation there has been quite an interesting first numerical

approach to solve the problem of critical bubbles with two Higgs fields [17]. In [15] the CP profile has been investigated in the background of a fixed Higgs profile. In [16] there are detailed investigations on CP-phases with restriction to a straight line between the minima.

The Euler Lagrange equations of (2) lead to the following set of coupled second order nonlinear differential equations

$$E_1 := \partial_\mu \partial^\mu \phi_1 + \phi_1 (\partial_\mu \theta)(\partial^\mu \theta) - \frac{\partial V_T(\phi_1, \phi_2, \theta)}{\partial \phi_1} = 0 \quad (5)$$

$$E_2 := \partial_\mu \partial^\mu \phi_2 - \frac{\partial V_T(\phi_1, \phi_2, \theta)}{\partial \phi_2} = 0 \quad (6)$$

$$E_3 := \partial_\mu(\phi_1^2 \partial^\mu \theta) - \frac{\partial V_T(\phi_1, \phi_2, \theta)}{\partial \theta} = 0. \quad (7)$$

The usual method for the SM case with only one Higgs field is to solve the corresponding single equation numerically by "turning around" the effective potential and dealing x for a time t. The problem then can be regarded as an initial value problem for the negative potential and one can use an overshooting-undershooting procedure. This works well since there is only one direction in field space.

This situation is completely different once there are additional directions in field space. Again one can consider the analogous mechanical problem with the turned around potential. Assuming that we do not have friction, the initial value problem is the same as trying to shoot a marble from one top of a hill (first minimum) to exactly the top of the other hill (second minimum) somewhere along the ridge in such a way that it comes to rest on the top of the second hill. Small changes in the initial conditions lead to a completely different shape of the solution. It is, in general, not possible to know the initial conditions with sufficient accuracy to find the desired solution.

Hence we have to devise another method. We here use the method of minimization of the functional of squared equations of motion. Constraining eqs. (5)-(7) to a stationary wall (domain wall) with velocity v_w at late time t where the wall is already almost flat we are left with only one spatial dimension $x = z - v_w t$ perpendicular to the wall. Then, solving eqs. (5)-(7) means finding field configurations for which

$$S_3 = \int_{-\infty}^{\infty} dx \left(E_1^2(x) + E_2^2(x) + E_3^2(x) \right) \quad (8)$$

is zero which is achieved by minimizing S_3. This method has also successfully been used in [17] for the critical bubble. The approach of [23] in principle also is a minimization procedure and therefore the following considerations are also applicable.

Using the minimization method we have to solve a boundary value problem. Thus we have to use an ansatz for every function for which we want to find the time development which fulfills the boundary conditions.
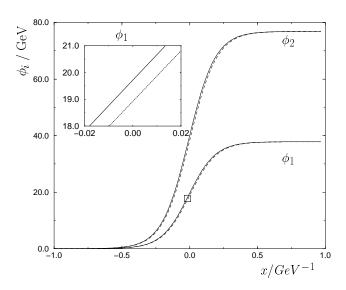

FIG. 1. Solution (solid) for the MSSM compared to kink-ansatz (dashed) for $m_A = 450$ GeV, $m_Q = 350$ GeV, $\tan \beta = 2.0$.

Our procedure works in two steps. The first step is to find an ansatz which is as close as possible to the exact solution. We will see that this is a crucial point. Throughout the literature we find the kink ansatz for the Higgs fields being quite appropriate. We therefore use for the N Higgs fields

$$\phi_i^{kink} = \frac{v_i}{2} \left(1 + \tanh(\frac{x}{L_i}) \right), \quad i = 1 \dots N \quad (9)$$

as our ansatz as well. The L_i are determined by minimizing (8). This first step is cheap in terms of computer time since it is only a N-dimensional minimization and can be performed very fast. Depending on the actual potential one may also introduce some further parameters like offsets $\hat{x}_i$ between the fields: $\phi_i = \frac{v_i}{2} \left(1 + \tanh(\frac{x}{L_i} + \hat{x}_i) \right)$. Minimizing with respect to a few parameters is a very successfull first step since it reduces the actual value of (8) already sigificantly compared to a general function which only fullfills the boundary conditions.

In figure 1 we show the solution in the MSSM for the simpler case where we have no CP violation ($\theta(x) = 0$) and the ansatz after this first step of our procedure is just the kink function $\phi_i(x) = \frac{v_i}{2}(1 + \tanh(\frac{x}{L_i}))$ with L_i now determined. We can recognize that in this case the minimizing kink function (solid lines) is already quite close to the actual solution (dashed lines). The shape of the tunneling valley strongly depends on the CP-odd Higgs mass m_A. Small m_A give a larger mixing with m_H and a sharper bending curve.

Unfortunately the kink ansatz does not serve as a general recipe. For example CP phases in general cannot be described very well by this ansatz and one would need further knowledge of their shape in the wall. For the critical bubble with small radius or potentials with sharper

2

curves the the ansatz 9 is not appropriate any more. One has to choose other types of functions as ansatz and, in addition, the second step becomes more important.

With this preoptimized ansatz we start the second step of our solving procedure, the high dimensional minimization. We use different numerical representations of the action (8) which in principle are discretizations of the variables over a grid. We afterwards compare the results obtained from different representations. In particular we have to discretize:

i) The space variable $x = z - v_w t$,

ii) the fields $\phi_i(x_j)$,

iii) the derivatives of the fields (first and second derivatives), and

iv) derivatives of explicitly given functions like the effective potential.

ad i) We use a grid of M points x_j, $\quad j = 1 \ldots M$. According to the special type of solution it is sometimes useful to transform the integration interval. E.g. for the kink ansatz which must be integrated over an infinite region it is useful to transform to $\phi_i(\tau)$ with $\tau = \frac{1}{2}(1 + \tanh(\frac{x}{L}))$ where $\tau \in [0, 1]$ which is a finite interval and has the advantage of many interpolation points where they are needed, in the transition range of the kink. We have compared this to a equidistant segmentation and obtained no important difference in the results. By adjusting the integration interval to the wall thickness L we take care that there are always enough interpolation points in the wall independent of L. The integration interval ranges between 5 and 10 times L. The regions outside of this interval do not contribute to (8) any more.

ad ii) The first and quite simple method is just to store the function values $\phi_i(x_j)$ into an array. To guarantee smoothness here we need many grid points. We have to store $N \times M$ variables for all fields.

The second approach is to interpolate the ansatz functions by smooth functions like splines. There are several types of splines (see refs. [24,25]). We use cubic splines, which are cubic polynomials through a given set of points with continous first and second derivative along the whole interpolation range. Moreover one can assign the derivatives at the endpoints of the curve which is useful for setting boundary conditions. For an interpolation here only relatively few points x_j are needed. Smoothness is guaranteed by definition. The price is an increase in computation time for each minimization step. "Nonlocality" also has another disadvantage: If a routine changes one point of the curve for finding a minimum it always changes a larger region of the curve which may cause eventually larger changes in (8) than useful and maybe, in the worst case, even a jump into another minimum. We use both approaches and compare the results.

ad iii) There are a lot of ways to discretize derivatives as finite difference equations connecting two or more grid points. We mostly use three- or four-point derivatives. Derivatives including more points may even impair the result since they require more additions and subtractions which are numerically problematic. Due to quite differ-ent orders of magnitude in the involved numbers they accummulate numerical errors. For this problem see also [24,26]. For derivative formulae see refs. [24,25]

ad iv) Finally the derivatives of explicitly given functions can be calculated explicitly as well as numerically. This depends on the problem. For potentials like the MSSM potential we found it to be sufficent to differenciate numerically.

The minimization itself is accomplished using Powell's method [24] to avoid further derivatives. Minimization parameters are the values $\phi_i(x_j)$ and $\theta(x_j)$ respectively. So with N fields defined at M grid points we have a $N \times M$-dimensional function to be minimized. Powell's method converges quadratically and can be used for very high dimensional minimizations (several hundred dimensions). Since Powell's method is comparably slow finding a minimum in an almost flat valley, it might be useful in such cases to combine it with a Newton's method (converging quadratically as well) or the like which has a good convergence behaviour as well. Roughly speaking, Powell's method finds valleys very fast and Newton's method finds the bottom of the minimum very fast. But the converse is not true in general. We also used downhill simplex minimization method for comparison which turned out to be much slowlier [24]. Other promising algorithms are "leap frog" and related methods [24,27].

Nevertheless there are still several undesired minima which can be categorized as follows:

a) Some are real solutions to the equations of motion. As an trivial example consider $\theta(x) = 0, \forall x$ which always is a solution to (5)-(7).

b) Fake minima due to the numerical representation of the functional. This is a common problem when including derivatives, discretized as finite differences.

c) Minimization of (8) is achieved by solving $\delta S = 0$. For a squared form $S = a^2$ in addition to the (desired) solution $a = 0$ also pseudo-solutions according to $\delta a = 0$ might exist.

There can also be combined effects between a), b) and c), e.g. one can have a pseudo-solution which is only found because of numerical "fluctuations" during the minimization procedure. The results often show oscillations at the outer integration regions (see figure 2). We found that this is a combination of a) and b) as we see from the analytical solution of the third equation of motion with small θ. Then the third equation decouples and at small x we have the reduced equation

$$\theta'' + \frac{4}{L}\theta' - |m_{12}^2| \tan\beta\theta = 0 \qquad (10)$$

which has the solution

$$\theta(x) = \exp\{-2x/L\} \cos(\omega x/L), \qquad (11)$$

a damped oscillation with frequency $\omega = \sqrt{4 - L^2|m_{12}^2| \tan\beta}$ and and growing amplitudes for $x \to -\infty$.
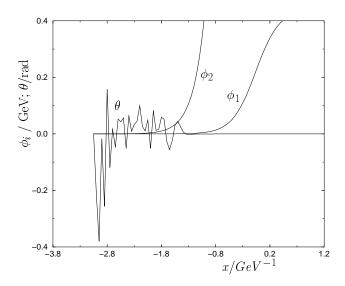
FIG. 2. Oscillation of an undesired solution of $\theta(x)$ near the origin, where θ is small and decouples from ϕ_1 and ϕ_2.
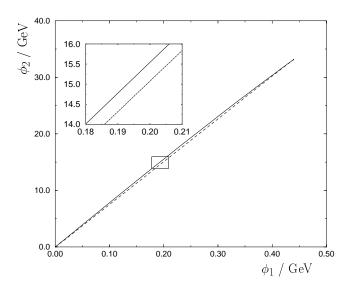

FIG. 3. Unphysically small values of $m_A \approx \mathcal{O}(10 \text{ GeV})$ demonstrate the deviation of the solution (solid) from the straight line (dashed).

This is what we find numerically. But since our boundary condition were $\theta'(\pm\infty)=0$ and we took as an ansatz the zero function $\theta(x) = 0$, we find this behaviour to be caused by the minimization routine. The routine came through a configuration around $\theta(x) = 0$. It differs inessentially from the ansatz but together with the chosen boundary conditions this configuration fits into the oscillation described above. Without this pseudo-solution $\theta(x)$ would remain zero for all x, as intended. Fortunately in the region of interest within the bubble $\theta(x)$ remains zero since the chosen parameters permit no CP violation there. This is typical for situations where an angle with vanishing moduli is not well defined any more.

Altogether this implies the possible problem that, starting from an ansatz which is in the vicinity of such an apparent solution, the algorithm might never converge to the desired exact solution. Therefore the importance of a good ansatz is obvious.

What can be done to avoid some of the problems and rate the quality of a minimum found? First we see that it is important to have a well prepared ansatz as near as possible to the desired solution to avoid reaching an unwanted local minimum after the time consuming second minimization step. As long as we have energy conservation, as in our example, one can check the quality of the results easily. It must be $T - V = 0$ or $T/V = 1$ and one can check the deviation. Here V is the QFT effective potential, the mechanical analog has the opposite sign, T is the kinetic energy density. It is possible to get results where T/V deviates only by few percent from 1.0. The energy check is already quite appropriate, it strongly depends on the quality of the solutions. It is not useful to add the energy conservation, which would be fullfilled by the real solution automatically, since it is another min-

imum finding task with all problems we have described. Only in the stationary case $T - V$ could actually be used instead of (8) whereas our method still holds in a more general case. One can think of further identities that have to be fulfilled, as in [23]. The described special behaviour of unwanted oscillations can be suppressed by restricting the parameter space of the minimization procedure at the boundaries. One can also increase the number of steps in the procedure to improve the precision step by step for the cost of computing time.

Since the kink solution is a good approximation to the bubble wall profile equations in a lot of models, we compared our result with [17]. In that paper the radial symmetric equations for the critical bubble were solved. Thus the solutions have a different shape but in field space there should be the same behaviour concerning the deviation from the straight line between the minima. And we indeed can confirm the results. $\Delta\beta$ is in the range of 10^{-3} to 10^{-2} for m_A around several hundred GeV [6,17]. Only for (experimentally excluded) small values of $m_A \approx \mathcal{O}(10\text{GeV})$ we find a considerable deviation from a straight line demonstrating a major deviation from the ansatz due to the minimization routine (see fig. 3).

CONCLUSIONS AND PROSPECT

In order to solve the phase transition problem for finding bubble wall solutions we presented a working algorithm. Often a simple ansatz like the kink turns out to be a good approximation. Especially in the 2HDM and the MSSM the deviations from this ansatz are small at least in some expressions like the surface tension. But for example for the baryon number asymmetry or the CP

violating phase this is not sufficient since these indeed depend on the small deviation from the simple ansatz: The latter would give zero for $\Delta\beta$. In some models this would prevent baryogenesis at all.

With our method we can confirm the results of [17] for the one loop MSSM effective action. The methods presented here can also be extended to investigate the dynamics of bubble expansion in more detail. For this we have to go beyond a constant critical temperature and include reactions of the bubble wall with a background fluid of particles as in [21]. These questions have to be studied further [28]. An investigation of the NMSSM with three Higgs fields and a stronger deviation from a straight line in field space is in progress as well.

[1] K. Rummukainen, M. Tsypin, K. Kajantie, M. Laine, M. Shaposhnikov, hep-lat/9805013

[2] D. Bödeker, P. John, M. Laine, M.G. Schmidt, Nucl. Phys. B497(1997)387

[3] M. Carena, M. Quirós, C.E.M. Wagner, Nucl. Phys. B524(1998)3

[4] M. Losada, hep-ph/9806519

[5] M. Laine, K. Rummukainen, Phys. Rev. Lett. 80(1998)5259, hep-lat/9804019

[6] J.M. Cline hep-ph/9810267; J.M. Cline, G.D. Moore, hep-ph/9806354 to appear in Phys. Rev. Lett.; G.D. Moore hep-ph/9801204, hep-ph/9805264

[7] A.D. Davies, C.D. Froggatt, R.G. Moorhouse, Phys. Lett. B372(1996)88; M. Pietroni, Nucl. Phys. B402(1993)27

[8] S.J. Huber, M.G. Schmidt, hep-ph/9809506

[9] A.G. Cohen, D.B. Kaplan, A.E. Nelson, Ann. Rev. Nucl. Sci. 43(1993)27

[10] V.A. Rubakov and M.E. Shaposhnikov, Usp. Fiz. Nauk 166(1996)493

[11] H. Davoudiasl, K. Rajagopal, E. Westphal, Nucl. Phys. B515(1998)384

[12] J.M. Cline, M. Joyce, K. Kainulainen, Phys. Lett. B417(1998)79

[13] D. Comelli, M. Pietroni, Phys. Lett. B306(1993)67

[14] A. Hammerschmitt, J. Kripfganz, M.G. Schmidt, Z. f. Phys. C64(1994)105

[15] J. Cline, K. Kainulainen, A.P. Visher, Phys. Rev. D54(1996)2451

[16] K. Funakubo, hep-ph/9809517; K. Funakubo, A. Kakuto, S. Otsuki, F. Toyoda hep-ph/9803444, K. Funakubo, hep-ph/9909517 & references therein

[17] J.M. Moreno, M. Quirós, M. Seco, Nucl. Phys. B526(1998)489

[18] M. Carena, M. Quirós, A. Riotto, I. Vilja, C.E.M. Wagner, Nucl. Phys. B503(1997)387

[19] M. Laine, Phys. Rev. D49(1994)3847; H. Kurki-Suonio, M. Laine, Phys. Rev. D54(1996)7163, Phys. Rev. Lett. 77 (1996) 3951

[20] K. Enqvist, J. Ignatius, K. Kajantie, K. Rummukainen, Phys. Rev. D45(1992)3415; J. Ignatius, K. Kajantie, H. Kurki-Suonio, M. Laine, Phys. Rev. D49(1994)3854

[21] G. Moore, T. Prokopec, Phys. Rev. D52(1995)7182, Phys. Rev. Lett. 75(1995)777

[22] A. Brignole, J.R. Espinosa, M. Quirós, F. Zwirner, Phys. Lett. B(1994)181

[23] A. Kusenko, Phys. Lett. B358(1995)47-50,51-55

[24] W. Press et al, *Numerical recipes*, Cambridge University Press 1988

[25] M. Abramowitz, I.A. Stegun, *Handbook Of Mathematical Functions With Formulas, Graphs and Mathematical Tables*, John Wiley & Sons, 1964,1972

[26] D. Knuth, *The Art of Computer Programming*, vol 2, Addison-Wesley, 2nd ed., 1981

[27] J.M. Cline, J.R. Espinosa, G.D. Moore, A. Riotto, hep-ph/9810261

[28] P. John, M. Laine, M.G. Schmidt, work in progress